encit 2020

ABCM Associação Brasileira de Engenharia e Ciências Mecânicas

18th Brazilian Congress of Thermal Sciences and Engineering
November 16–20, 2020 (Online)

ENCIT2020-0367
Development of a Transient Model for Fluid Flow, Heat Transfer and Pressure Buildup in Wellbores

Ianto Oliveira Martins
Arthur Pandolfo da Veiga
Eduardo Bader Dalfovo Mohr Alves
Alexandre Kupka da Silva
Jader Riso Barbosa Jr
Departamento de Engenharia Mecânica
Universidade Federal de Santa Catarina
ianto.oliveira@polo.ufsc.br
arthur.veiga@polo.ufsc.br
eduardo.alves@polo.ufsc.br
a.kupka@ufsc.br
jrb@polo.ufsc.br
A. Rashid Hasan
Department of Petroleum Engineering
Texas A&M University
rashid.hasan@tamu.edu

Abstract. *Annular Pressure Buildup (APB) can occur in most operating wellbores experiencing significant thermal gradient with respect to the adjacent formation. It is defined as the pressure increase caused by the thermal expansion of a fluid in sealed annuli. The present work presents a fully coupled thermo-hydraulic model to estimate temperature and pressure profiles inside a well, as well as estimating the pressure buildup inside each annulus. The model consists of momentum and energy differential balances for each vertical layer of the well, as well as an equation to determine the structural deformation of the well and the calculation of the APB itself. All the equations were discretized using the finite difference model, implemented on Python 3 and solved with a builtin package. A production wellbore was simulated for the period of 10 days and the APB calculated for this period of time was 50* MPa*, highlighting the necessity of a computational tool to estimate the scale of the phenomenon. A parametric study was also performed considering the variation of inlet variables, such as temperature, pressure, liquid flow rate and GOR.*

Keywords: *Wellbore, Annular Pressure Buildup, Transient, Heat Transfer, Numeric method*

1. INTRODUCTION

Wellbore temperature increase is a serious issue in offshore wells. As the high-temperature hydrocarbons flow from the reservoir towards the wellhead, the entire wellbore is heated up and the expansion of the fluids trapped inside the concentric annuli raises their pressure. The phenomenon of APB (Annular Pressure Buildup) has been associated with collapsing incidents during drilling operations (Pattillo *et al.*, 2004).

Heat and momentum transfer in oil production and injection wells have been studied since the work of Ramey Jr (1962). The hypotheses considered in his pioneering work were single-phase injection fluid, constant thermophysical properties for all the materials in the well. More importantly, the well was treated as an infinite line source with a constant heat flux boundary condition, which is known to overestimate the fluid temperature for short time operations. Since then, other methods have been developed to estimate the heat flux between the wellbore and the surrounding formation considering different scenarios (Chiu and Thakur, 1991), shorter times (Hasan and Kabir, 1991), and formation properties (Cheng *et al.*, 2011).

Technological advances resulting from improvements of computational methods and hardware allowed the development of transient models at a reasonable computational cost. One example is the work of Yi *et al.* (2018), where the transient injection of supercritical carbon dioxide was simulated with the additional consideration of temperature- and pressure-dependent thermophysical properties of the injection fluid. However, the authors did not disclose how the temperature at the interface with the formation was calculated. Other authors, such as Gao *et al.* (2017), have coupled the wellbore thermal model to a two-dimensional heat transfer model to estimate the temperature distribution in the surround-

ing formation.

A precise temperature estimation is fundamental to the correct prediction of APB, mainly in the case of offshore wells, where venting the annulus to release the trapped fluid is not an option. Therefore, the present work aims to develop a transient model to estimate temperature and pressure profiles in a production wellbore, as well as the APB behavior. The simulation considers the thermal capacity of the concentric layers of the wellbore, as well as the dependence of the thermophysical properties of the fluid layers with respect to temperature and pressure.

2. WELL GEOMETRY AND CHARACTERISTICS

Figure 1 is an axysimmetric view of the of the simulated wellbore. All annuli are sealed, so no fluid leaks are considered. Annulus A is modelled as a 20/80 wt.% mass mixture of salt and water (brine); annuli B and C were modelled as a 50/50 wt.% mixture of water and glycol.

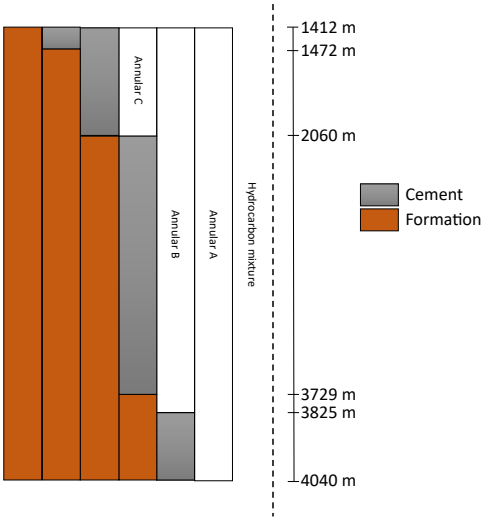

Figure 1: Schematic geometry of the wellbore

Table 1 complements Fig. 1 with the geometric details and dimensions of the wellbore. It is worth noting that the well was separated into vertical layers containing each material and each one of these layers represents a concentric cylinder shell, except for the first one, which is a full cylinder. How this geometric discretization ties into the mathematical model will be explained at the next section.

The inlet point of the fluid flow is located at the bottom of first layer, i.e., $z = 4040\ \mathrm{m}$, and the outlet point is located at the wellhead, i.e., $z = 1412\ \mathrm{m}$. The formation temperature gradient is $0.044\ \mathrm{K\,m^{-1}}$, with a seabed temperature of 277.15 K and the annuli initial gradient is $22.1\ \mathrm{MPa}$. The initial temperature profile and well inclination are shown by Fig. 2.

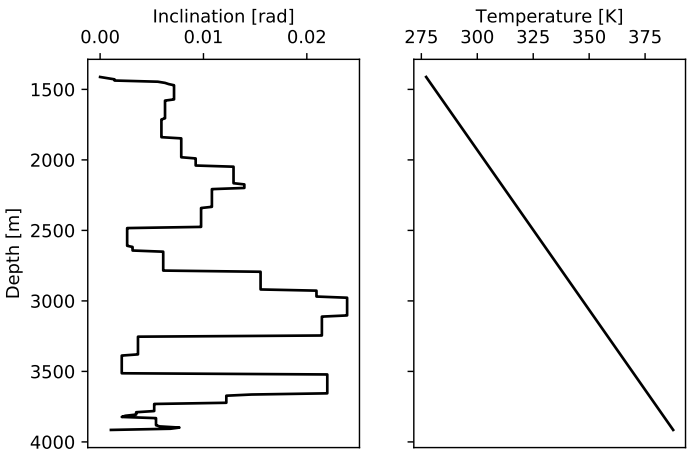

Figure 2: Well inclination and initial temperature profile

Table 1: Geometric characteristics of the wellbore

Layer	Range [m]	Material	Radius [m]
1	1412 - 4040	Hydrocarbon mixture	0.075
2	1412 - 4040	Carbon steel	0.084
3	1412 - 4040	Annular A	0.121
4	1412 - 4040	Carbon steel	0.137
5	1412 - 3729	Annular B	0.157
	3729 - 3825		0.187
	3825 - 4040	Cement	0.187
6	1412 - 3729	Carbon steel	0.170
	3729 - 4040	Formation	0.188
7	1412 - 1437	Annular C	0.229
	1437 - 2040		0.238
	2040 - 2060		0.203
	2060 - 3729	Cement	0.203
	3729 - 4040	Formation	0.203
8	1412 - 2040	Carbon steel	0.254
	2040 - 4040	Formation	0.254
9	1412 - 1437	Cement	0.343
	1437 - 1472		0.356
	1472 - 2060		0.330
	2060 - 4040	Formation	0.330
10	1412 - 1472	Carbon steel	0.381
	1472 - 4040	Formation	0.381
11	1412 - 1472	Cement	0.457
	1472 - 4040	Formation	0.457

3. MATHEMATICAL MODEL

The main hypotheses of the mathematical model are as follows:

1. Constant thermophysical properties for the solid components
2. Pseudo steady-state momentum transfer for the production fluid flow in the central tubing
3. Transient heat transfer in the well and surrounding formation
4. Deformation of the solid components do not affect the momentum and energy balances
5. The annuli are sealed (no leaks between annuli and the formation).

Since the characteristic time of the flow is lower than the timestep of the simulation, it is safe to assume a quasi-steady regime for the momentum balance resulting in the Eq. (1).

$$\frac{\mathrm{d}p}{\mathrm{d}z} = -\rho g \sin\theta - f\frac{\rho v^2}{4r} - \rho v \frac{\mathrm{d}v}{\mathrm{d}z} \tag{1}$$

where p is fluid pressure (Pa), ρ is density ($\mathrm{kg\,m^{-3}}$), g is gravity acceleration($\mathrm{m\,s^{-2}}$), θ is the angle of inclination between well and lower surface (rad), f is friction factor ($-$) calculated by Colebrook *et al.* (1939), v is fluid flow velocity ($\mathrm{m\,s^{-1}}$), r is tubing radius (m) and z is the distance from the seabed (m).

Equation (2) is the energy balance for the wellbore. It is important to note that each layer of the wellbore has a differential equation to calculate its temperature, with the subscript i indicating the layer (which can be a fluid or a solid).

$$\rho_i c_{p,i}\frac{\partial T_i}{\partial t} + \rho_i c_{p,i} v_i \frac{\partial T_i}{\partial z} = \frac{\partial}{\partial z}\left(k_i \frac{\partial T_i}{\partial z}\right) + \frac{T_{i+1} - T_i}{R_{i/i+1}V_i} - \frac{T_i - T_{i-1}}{R_{i-1/i}V_i} + (1 + \rho_i \gamma_{J,i} c_{p,i})\left(\frac{\partial p_1}{\partial t} + v_i \frac{\partial p_1}{\partial z}\right) + \frac{\rho_i f_i v_i^3}{4r_i} \tag{2}$$

where c_p is specific heat ($\mathrm{J\,kg^{-1}\,K^{-1}}$), T is temperature (K), k is thermal conductivity ($\mathrm{W\,m^{-1}\,K^{-1}}$), R is radial thermal resistance ($\mathrm{K\,W^{-1}}$), V is volume ($\mathrm{m^3}$), γ_J is Joule-Thomson coefficient ($\mathrm{K\,Pa^{-1}}$) and t is time (s).

As mentioned above, the temperature is calculated at the center of each control volume, therefore, the resistance between two adjacent nodes is a combination of the thermal resistances between each node and the interface between the two layers. The conduction and convection thermal resistances are calculated according to the following equations:

$$R = \frac{\ln \frac{r_{out}}{r_{in}}}{2\pi L k} \tag{3a}$$

$$R = \frac{1}{2\pi r L h} \tag{3b}$$

where h is the convective heat transfer coefficient ($\mathrm{W\,m^{-2}\,K^{-1}}$) (Sieder and Tate, 1936). Equations (4), (5), (6) and Eq. (7) calculate the energy balance at the production fluid, tubing, intermediate layers and the last layer, respectively.

$$\rho_1 c_{p,1}\frac{\partial T_1}{\partial t} + \rho_1 c_{p,1} v_1 \frac{\partial T_1}{\partial z} - \frac{2h\left(T_2 - T_1\right)}{r_1} = \left(1 + \rho_1 \gamma_{J,1} c_{p,1}\right)\left(\frac{\partial p_1}{\partial t} + v_1 \frac{\partial p_1}{\partial z}\right) + \frac{\rho_1 f v_1^3}{4 r_1} \tag{4}$$

$$\rho_2 c_{p,2}\frac{\partial T_2}{\partial t} - \frac{\partial}{\partial z}\left(k_2 \frac{\partial T_2}{\partial z}\right) + \frac{2 r_1 h\left(T_2 - T_1\right)}{r_2^2 - r_1^2} - \frac{2 k_2 k_3 \left(T_3 - T_2\right)}{\left(k_3 \ln \frac{2 r_2}{r_1 + r_2} + k_2 \ln \frac{r_2 + r_3}{2 r_2}\right)\left(r_2^2 - r_1^2\right)} = 0 \tag{5}$$

$$\rho_i c_{p,i}\frac{\partial T_i}{\partial t} - \frac{\partial}{\partial z}\left(k_i \frac{\partial T_i}{\partial z}\right) + \frac{2 k_{i-1} k_i \left(T_i - T_{i-1}\right)}{\left(k_{i-1} \ln \frac{r_{i-1} + r_i}{2 r_{i-1}} + k_i \ln \frac{2 r_{i-1}}{r_{i-2} + r_{i-1}}\right)\left(r_i^2 - r_{i-1}^2\right)} - \frac{2 k_i k_{i+1} \left(T_{i+1} - T_i\right)}{\left(k_{i+1} \ln \frac{2 r_i}{r_{i-1} + r_i} + k_i \ln \frac{r_i + r_{i+1}}{2 r_i}\right)\left(r_i^2 - r_{i-1}^2\right)} = 0 \tag{6}$$

$$\rho_i c_{p,i}\frac{\partial T_i}{\partial t} - \frac{\partial}{\partial z}\left(k_i \frac{\partial T_i}{\partial z}\right) + \frac{2 k_{i-1} k_i \left(T_i - T_{i-1}\right)}{\left(k_{i-1} \ln \frac{r_{i-1} + r_i}{2 r_{i-1}} + k_i \ln \frac{2 r_{i-1}}{r_{i-2} + r_{i-1}}\right)\left(r_i^2 - r_{i-1}^2\right)} - \frac{2 k_i k_e \left(T_{e,o} - T_i\right)}{\left(k_e \ln \frac{2 r_i}{r_{i-1} + r_i} + \mathrm{f}\left(t\right) k_i\right)\left(r_i^2 - r_{i-1}^2\right)} = 0 \tag{7}$$

where $\mathrm{f}\left(t\right)$ is the dimensionless time function $(-)$ (Hasan and Kabir, 1991). The natural convection will be considered in the fluid layers by employing the correction for the thermal conductivity proposed by Zhou (2013).

The APB for a given annulus at a given time is defined as the pressure change with respect to a reference (initial) time:

$$\Delta p_i = p_i^* - p_{i,0}^* \tag{8}$$

The pressure, p_i^*, is determined by solving the following mass conservation in the annulus:

$$\frac{m_i}{V_i} - \rho_i\left(\bar{T}_i, p_i^*\right) = 0 \tag{9}$$

where m is the mass of fluid in the annulus (kg), V is the annulus volume($\mathrm{m^3}$), $\bar{T}$ is average temperature (calculated based on the temperature profiled results from the thermal model) (K), and ρ is the mass density computed using an equation of state for the compressed liquid as a function of pressure and temperature ($\mathrm{kg\,m^{-3}}$).

The volume of the annular cavity may change during operation, due to thermal expansion of the casing and structural deformation resulting from an imbalance between external and internal forces acting on the annulus. In Eq. (9), the volume term, V_i, is recalculated at every timestep to consider this deformation. The deformation model implemented is the one developed by Halal and Mitchell (1994).

3.1 Numerical Model

The numerical method employed in the discretization of all equations was the backward finite difference method. All the layers were equally refined and the temperature for all the layers were simultaneously obtained, eliminating the need for iterative loops to couple all equations. Nevertheless, iterative loops were required to consider the temperature and pressure effects upon the thermophysical properties of the fluids.

Figure 3 presents the mesh employed in the simulation, along with the boundary conditions. The figure also highlights the use of a dimensionless time function, f(t) (Hasan and Kabir, 1991), being employed at the resistance between the last layer of the well and the formation.

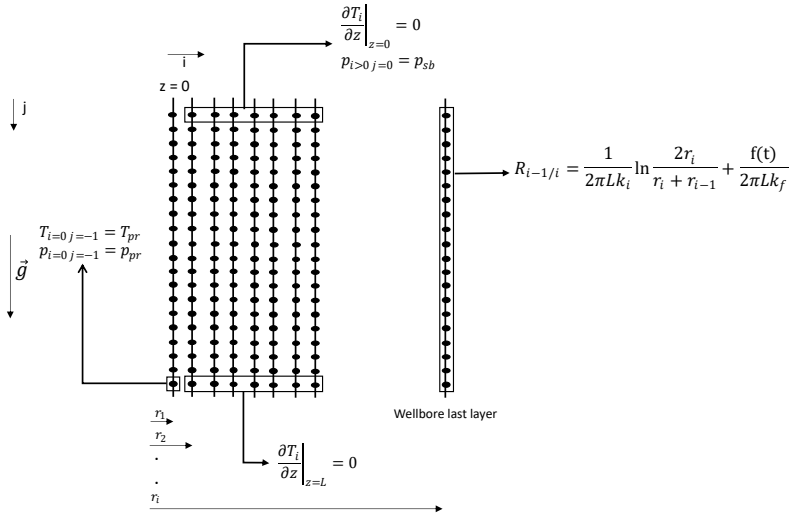

Figure 3: Simulation mesh

Thermophysical properties of the fluid materials were calculated using a commercial software (Infochem/KBC, 2018). All the calculations were performed in a custom made routine developed with Python 3 (Van Rossum and Drake, 2009).

3.2 Simulation parameters

The influence of the inlet production parameters will be studied in this work. In total, 9 simulations were made, which are shown in Tab. 2. Simulation # 1 will be taken as a standard condition for the comparisons; in Tab. 2 the varying parameters are liquid flow rate (# 2 and # 3), pressure (# 4 and # 5), gas-oil ratio (# 6 and # 7) and temperature (# 8 and # 9).

Table 2: Simulation parameters

Simulation	Liquid flow rate [$\mathrm{m^3\,s^{-1}}$]	Temperature [K]	Pressure [MPa]	Gas-Oil Ratio [$-$]
# 1	0.017	396.8	31.0	211
# 2	0.034	396.8	31.0	211
# 3	0.009	396.8	31.0	211
# 4	0.017	396.8	37.0	211
# 5	0.017	396.8	25.0	211
# 6	0.017	396.8	31.0	422
# 7	0.017	396.8	31.0	105
# 8	0.017	410.8	31.0	211
# 9	0.017	376.8	31.0	211

4. RESULTS

4.1 Parametric Analysis

Simulation # 1 will be taken as a standard simulation for the next comparisons. Figure 4 presents a comparison between the simulations for the production fluid, with a total time of 1 day; the results were grouped based on the parameter changed.

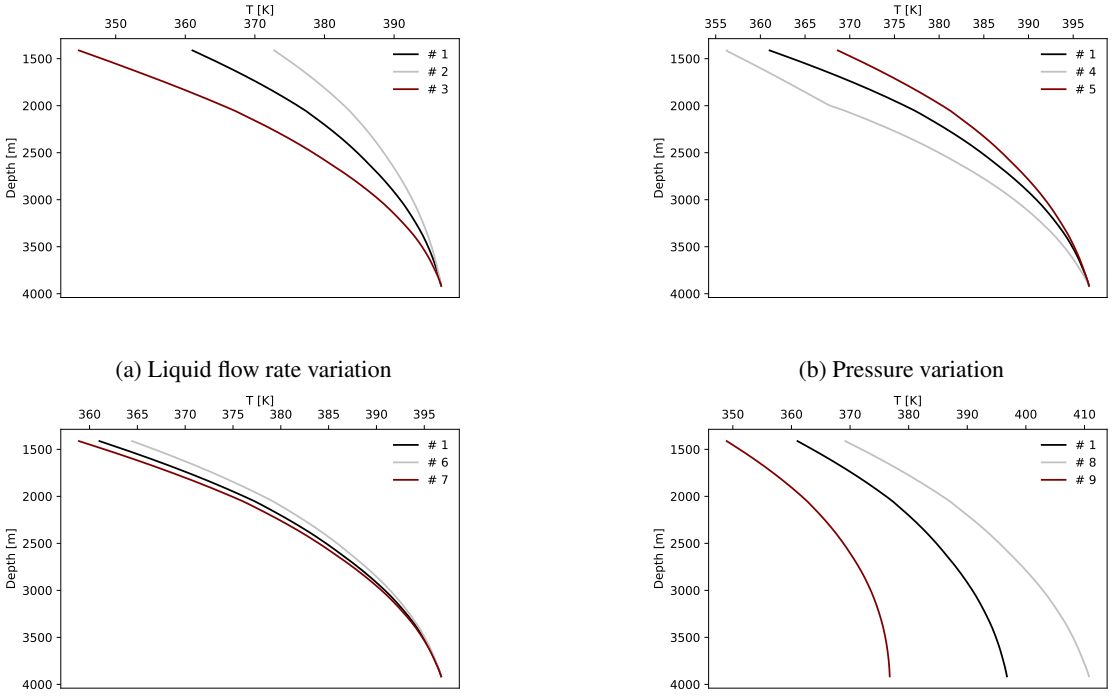

(a) Liquid flow rate variation

(b) Pressure variation

(c) Gas-Oil Ratio variation

(d) Temperature variation

Figure 4: Temperature profiles for the production fluid after 1 day

In Fig. 4a the result indicates that with a higher production rate the heat loss of the production fluid will be reduced; an explanation for this result is the lower residence time of the fluid flow, i.e., an element entering the production line will remain a shorter time inside the well losing heat to the rest of the well, losing less energy radially. In Fig. 4b, a higher pressure will cause the temperature at the wellhead to be lower than the other cases; the pressure gradient influence on the production fluid temperature is on the vapor quality of the production fluid: higher pressures will lead to increased vapor quantities, leading to a higher energy loss and reduced temperatures. In Fig. 4c, the gas-oil ratio is shown to have a reduced influence in the overall temperature profile; higher values will lead to higher temperatures near the wellhead, this can be explained that higher values of GOR increase the mixture velocity and reduce the heat loss in the well. Figure 4d shows the influence of the inlet temperature at the temperature profiles; temperature does not have a large influence in the vapor quality profile and the three curves are parallel, differing in a fixed value.

Figure 5a presents the APB profiles in Annular A for all the simulations; simulations # 8 and # 9 represent both extremes after 1 day of production, indicating that the inlet production fluid temperature has a higher influence in the APB calculation than any other of the studied variables. The APB curve for simulation # 2 has a higher inclination at the beginning of the simulation, indicating a higher heating rate of the annular fluid than the other simulations. Figure 5b has a similar pattern as Fig. 5a, with both extremes being the results of simulations # 8 and # 9, albeit the APB increase occurs at a lower rate, which can be inferred that is because the annulus B fluid is heated at a lower rate than annular A fluid. Figure 5c shows a different pattern than the observed at the other annuli: the variable with the most influence at the time of 1 day is the liquid flow rate; this can be explained with the distance between this annulus and the production fluid, the higher the distance, higher will be the thermal resistance between these layers, hence, the heating rate will be slower. It can also be inferred from the low inclination of the APB curve through time a reduced heating rate. Other interesting factor is that for 1 day the APB curve in Annular C still has a rising tendency, even though its value is similar to the APB in Annular B, which enables the prediction that for longer times the APB in Annular C will outgrow the APB in Annular B.

4.2 Standard Simulation for 10 Days

The evolution of the temperature at the wellhead during 10 days of simulation # 1 is shown in Fig. 6. After 2 days there is a stabilization of the temperature at the wellhead and a clear relation can be established with the APB profile, seen in Fig. 7, which presents the APB profiles after 10 days of production. As previously expected, after 10 days the APB at annulus C increased more than that of Annular B but a common trend among all is that after 10 days the APB is increasing at a reduced rate than it was at the start of the operation.

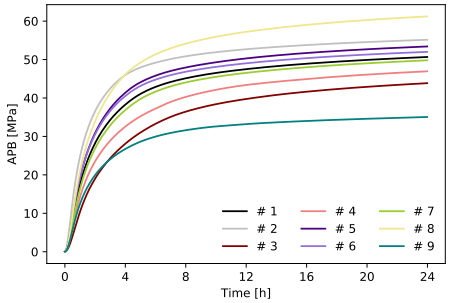

(a) Annular A

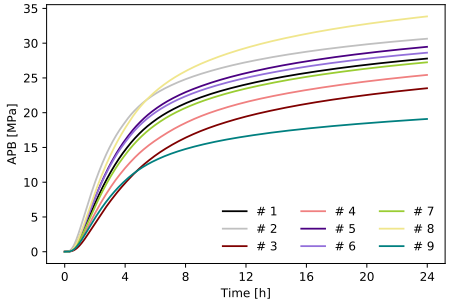

(b) Annular B

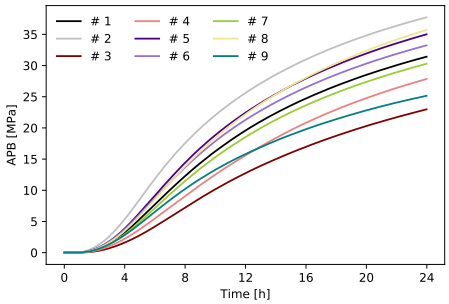

(c) Annular C

Figure 5: Annular Pressure Buildup

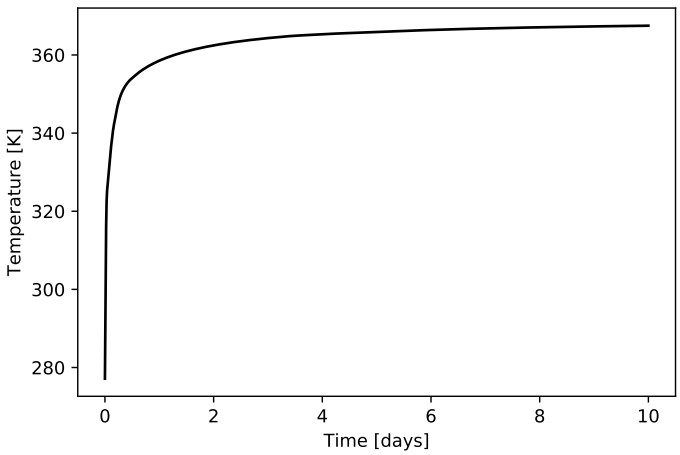

Figure 6: Temperature at the wellhead

Temperature and pressure profiles for both 1 and 10 days are shown in Fig. 8. As expected for a production operation, the entire well is heated during the process, after 1 and 10 days of operation the temperature at the wellhead rose 84 and 91 K, respectively. Figures 8a and 8b show that the temperature of closer layers to the production fluid increases at a higher rate. These figures also presents the pressure profiles, considering the APB. In Fig. 8a the pressure gradient at annuli B and C is similar, due to these two annuli being filled with the same fluid and having a similar APB, seen in Fig. 7. In Fig. 8b the discontinuities present in the temperature curves are due to the changing thermophysical properties of the fluids and the discontinuity itself of the adjacent solid layers.

5. CONCLUSION

The transient method can be employed to calculate temperature, pressure and pressure buildup for every instant of the simulation, unlike the pseudo-transient commonly employed by the industry and commercial softwares.

A parametric analysis showed the influence that production parameters such as temperature and pressure have on the

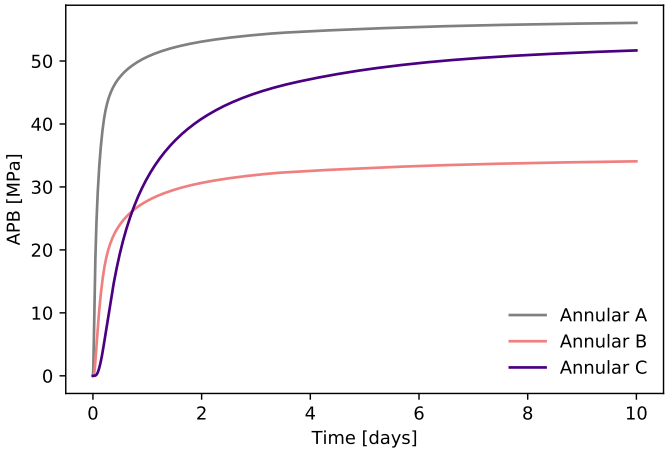

Figure 7: APB for all annuli

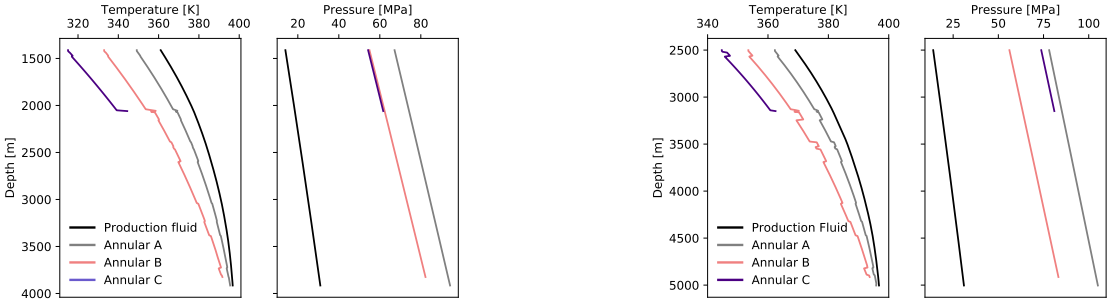

(a) 1 day of production

(b) 10 days of production

Figure 8: Pressure and temperature profiles

generated APB. Since APB needs to be considered in the well project, for safety measures, a robust mathematical model is essential; the one presented in this work considered several different phenomena, such as the transient behavior, fluids properties dependance upon temperature and pressure and structural deformation. The transient model can also be used as a tool for live monitoring of the operation temperature and pressure.

6. ACKNOWLEDGEMENTS

The authors would like to acknowledge CNPq for the financial support and Petrobras for the financial and technical support.

7. REFERENCES

Cheng, W.L., Huang, Y.H., Lu, D.T. and Yin, H.R., 2011. "A novel analytical transient heat-conduction time function for heat transfer in steam injection wells considering the wellbore heat capacity". *Energy*, Vol. 36, No. 7, pp. 4080–4088.

Chiu, K. and Thakur, S., 1991. "Modeling of wellbore heat losses in directional wells under changing injection conditions." In *SPE Annual Technical Conference and Exhibition*. Society of Petroleum Engineers.

Colebrook, C.F., Blench, T., Chatley, H., Essex, E., Finniecome, J., Lacey, G., Williamson, J. and Macdonald, G., 1939. "Correspondence. turbulent flow in pipes, with particular reference to the transition region between the smooth and rough pipe laws.(includes plates)." *Journal of the Institution of Civil engineers*, Vol. 12, No. 8, pp. 393–422.

Gao, Y., Sun, B., Xu, B., Wu, X., Chen, Y., Zhao, X., Chen, L. *et al.*, 2017. "A wellbore/formation-coupled heat-transfer model in deepwater drilling and its application in the prediction of hydrate-reservoir dissociation". *SPE journal*, Vol. 22, No. 03, pp. 756–766.

Halal, A.S. and Mitchell, R., 1994. "Casing design for trapped annular pressure buildup". *SPE Drilling & Completion*, Vol. 9, No. 02, pp. 107–114.

Hasan, A. and Kabir, C., 1991. "Heat transfer during two-phase flow in wellbores; part i–formation temperature". In *SPE Annual Technical Conference and Exhibition*. Society of Petroleum Engineers.

Infochem/KBC, 2018. "Multiflash^{TM} v7.0." URL `https://www.kbc.global/`. Accessed: 2019-01-30.

Pattillo, P.D., Cocales, B.W., Morey, S.C. *et al.*, 2004. "Analysis of an annular pressure buildup failure during drill ahead". In *SPE Annual Technical Conference and Exhibition*. Society of Petroleum Engineers.

Ramey Jr, H.J., 1962. "Wellbore heat transmission". *Journal of petroleum Technology*, Vol. 14, No. 04, pp. 427–435.

Sieder, E.N. and Tate, G.E., 1936. "Heat transfer and pressure drop of liquids in tubes". *Industrial & Engineering Chemistry*, Vol. 28, No. 12, pp. 1429–1435.

Van Rossum, G. and Drake, F.L., 2009. *Python 3 Reference Manual*. CreateSpace, Scotts Valley, CA. ISBN 1441412697.

Yi, L.P., Li, X.G., Yang, Z.Z. and Sun, J., 2018. "Coupled calculation model for transient temperature and pressure of carbon dioxide injection well". *International Journal of Heat and Mass Transfer*, Vol. 121, pp. 680–690.

Zhou, F., 2013. *Research on heat transfer in geothermal wellbore and surroundings*. PhD dissertation, Technischen Universität Berlin, Berlin.

RESPONSIBILITY NOTICE

The authors are solely responsible for the printed material included in this paper.